Electronic structures and elastic properties of monolayer and bilayer transition metal dichalcogenides MX_2 (M = Mo, W; X = O, S, Se, Te): A comparative first-principles study*

Zeng Fan(曾 范)[a)b)c)], Zhang Wei-Bing(张卫兵)[b)†], and Tang Bi-Yu(唐壁玉)[a)c)‡]

[a)] *Department of Physics, Xiangtan University, Xiangtan* 411105, *China*

[b)] *School of Physics and Electronic Sciences, Changsha University of Science and Technology, Changsha* 410114, *China*

[c)] *School of Chemistry and Chemical Engineering, Guangxi University, Nanning* 530004, *China*

(Received 25 March 2015; revised manuscript received 24 April 2015; published online 20 July 2015)

First-principle calculations with different exchange-correlation functionals, including LDA, PBE, and vdW-DF functional in the form of optB88-vdW, have been performed to investigate the electronic and elastic properties of two-dimensional transition metal dichalcogenides (TMDCs) with the formula of MX_2(M = Mo, W; X = O, S, Se, Te) in both monolayer and bilayer structures. The calculated band structures show a direct band gap for monolayer TMDCs at the K point except for MoO_2 and WO_2. When the monolayers are stacked into a bilayer, the reduced indirect band gaps are found except for bilayer WTe_2, in which the direct gap is still present at the K point. The calculated in-plane Young moduli are comparable to that of graphene, which promises possible application of TMDCs in future flexible and stretchable electronic devices. We also evaluated the performance of different functionals including LDA, PBE, and optB88-vdW in describing elastic moduli of TMDCs and found that LDA seems to be the most qualified method. Moreover, our calculations suggest that the Young moduli for bilayers are insensitive to stacking orders and the mechanical coupling between monolayers seems to be negligible.

Keywords: transition metal dichalcogenides, bilayer structures, elastic properties, electronic structure

PACS: 71.15.Nc, 62.20.de, 62.20.dj, 73.22.–f **DOI:** 10.1088/1674-1056/24/9/097103

1. Introduction

The successful isolation of graphene has brought in great revolutions for the modern material sciences.[1] The fascinating properties, such as the exceptionally high electron mobility ($\sim 10^5$ cm$^2\cdot$V$^{-1}\cdot$s^{-1})[2] and unique combination of high modulus ($\sim$ 1000 GPa) and tensile strength ($\sim$ 100 GPa),[3] have made graphene one of the most promising candidates for future flexible and stretchable electronics. However, the lack of band gap in pristine graphene limits its applications in reality. Due to the presence of a sizeable direct band gap in the visible frequency range,[4,5] two-dimensional transition metal dichalcogenides (TMDCs) monolayers have been recently suggested as an important candidate for electronic and optoelectronic devices.[4–6] Meanwhile, TMDCs also exhibit a number of intriguing optical phenomena such as valley-selective circular dichroism and the rich physics associated with the valley degree of freedom.[7] Moreover, their band gaps are tunable with thickness and different monolayer TMDCs can also be reassembled into designer van der Waals heterostructures,[8] which may lead to even richer physics and device applications.

Mechanical properties of materials such as elastic modulus are of vital importance in any practical device applications. It is thus a necessary prerequisite for the integration of TMDCs in various devices to obtain a detailed knowledge of mechanical properties of monolayer and two-dimensional (2D) heterostructures. Using nanoindentation in an atomic force microscope, Bertolazzi *et al.*[9] have investigated in-plane stiffness and breaking strength of suspended monolayer and bilayer MoS_2, which indicated that monolayer MoS_2 exhibits exceptional mechanical properties comparable to stainless steel. In-plane stiffness of monolayer and bilayer MoS_2 were found to be 180±60 N$\cdot$m^{-1} (corresponding to an effective Young's modulus of 270±100 GPa) and 260±70 N$\cdot$m^{-1} (200±60 GPa), respectively. Recently, the elastic moduli of CVD grown monolayer MoS_2 and WS_2 and their bilayer heterostructures were also investigated.[10] High 2D elastic moduli of CVD monolayer MoS_2 and WS_2 ($\sim$ 170 N$\cdot$m^{-1}) were also found. The 2D moduli of their bilayer heterostructures were found to be lower than the sum of 2D modulus for each layer, which shows a strong mechanical interlayer coupling between the layers.[10]

The importance of mechanical properties in future device applications also intrigues theoretical interest. The in-plane stiffness of monolayer MoS_2 has been investigated extensively.[11–15] However, the scattered theoretical results

*Project supported by the Construct Program of the Key Discipline in Hunan Province, China and Aid Program for Science and Technology Innovative Research Team in Higher Educational Institutions of Hunan Province, China.

†Corresponding author. E-mail: zhangwb@csust.edu.cn

‡Corresponding author. E-mail: tangbiyu@gxu.edu.cn

© 2015 Chinese Physical Society and IOP Publishing Ltd

from 124 to 146 N·m^{-1} seems to be lower than the experimental value of 170 N·m^{-1}. Recently, the in-plane stiffness of a series of monolayer MX_2 (M = Mo, W; X = S, Se, Te, O) has also been investigated by Kang *et al.*[13] and Çakr *et al.*[14] Their results suggested that TMDCs with W (O) atom are found to be much stiffer in each chalcogenide (metal) group. It should be noticed that the Young modulus of TMDCs obtained using PBE functional seems to be lower than the experimental measure as shown above, it is thus interesting to evaluate the performance of commonly-used functionals to describe the mechanical properties of TMDCs. On the other hand, in contrast to the extensive studies for monolayers, elastic and mechanical properties of bilayer TMDCs are still lacking completely. Previous study has suggested a transition from direct gap in the monolayer to indirect gap in the bilayer for TMDCs,[4,16–18] which implies a strong electronic coupling between different monolayers in bilayer TMDCs. Meanwhile, stacking order is also found to affect the electronic band structure and absorption spectra.[19] It is thus quite interesting to investigate mechanical coupling between monolayers and to reveal the role of stacking order on the elastic property of bilayer TMDs theoretically.

To understand the electronic and mechanical coupling of monolayers in bilayer TMDCs, we have investigated electronic and elastic properties of eight kinds of TMDCs in both monolayer and bilayer structures, in which different functionals are employed for comparison. The detailed structures, electronic properties, elastic constants, and Young moduli of TMDCs both in monolayer and bilayer obtained using LDA, PBE, and optB88-vdW functional are given and compared with the available experimental and theoretical results. Moreover, the performance of different functionals in describing the elastic properties of TMDCs is also evaluated.

2. Computational details

The present calculations were performed with the *Vienna ab-initio* simulation package (VASP) code[20,21] within the projector augmented wave (PAW) method. The local density approximation (LDA) and Perdew–Burke–Ernzerhof (PBE) were used in our calculation for comparison. To take into account van der Waals forces, which are expected to play a crucial role in the bilayer, the van der Waals density functional in the form of optB88-vdW[22,23] was used. Recent study has evidenced that the optB88-vdW can give much improved results for the graphene/metal surface.[24] Cut off energy and Brillouin zone (BZ) sampling were determined after an extensive convergence test. The Brillouin zone was simplified by an (18×18×1) Monkhorst–Pack grid and a plane-wave basis set with kinetic cutoff energy of 550 eV was applied. The atomic positions of those 2D TMDCs have been optimized by using the conjugate-gradient (CG) algorithm. A vacuum of 20 Å was set to prevent interactions between periodic images. The elastic constants were obtained by strain–energy method. By applying a set of suitable deformations to the single unit cell of the 2D TMDCs, we obtained the energy–strain curves and the corresponding elastic constant. The detailed relationships between the applied strain and the elastic constant have been shown in Ref. [25]. The strains ranging from −0.05 to 0.05 in steps of 0.01 were used in the present calculation.

3. Results and discussion

3.1. Monolayer TMDCs

3.1.1. Structure properties

The structure of monolayer TMDCs is shown in Fig. 1(a), in which the M and X atoms occupy the hexagonal honeycomb site alternately. Due to the chemical ratio of $M : X$ = 1:2, the M sublattice layer is sandwiched between two nearby X sublattice layers and forms an X–M–X covalently bonded hexagonal quasi-2D lattice as shown in Fig. 1(b), rather than the planar construction of the graphene.

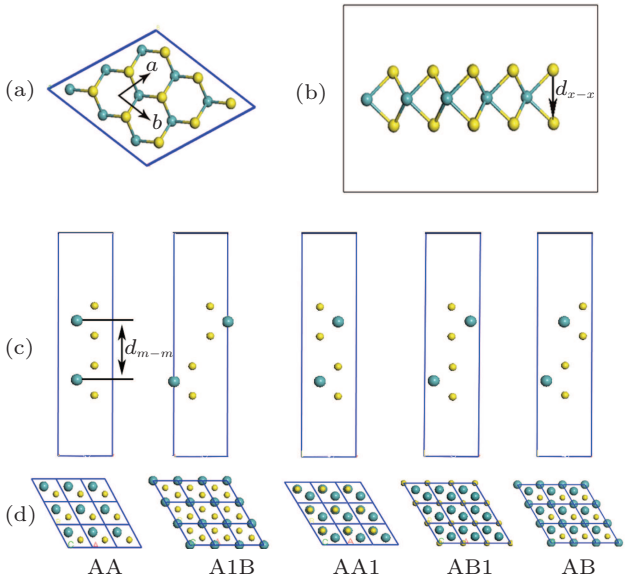


Fig. 1. (color online) Top view (a) and side view (b) of the monolayer TMDCs. Panels (c) and (d) are stacking structures for bilayer. Yellow balls and green balls represent metal and chalcogen atoms respectively. Here, d_{x-x} and d_{m-m} mean the bond lengths of two X atoms and two M atoms, respectively.

The optimized structural parameters of TMDCs with LDA, PBE, and optB88-vdW methods are listed in Table 1, two previous PBE calculations[13,14] are listed for comparison. We can find that the previous calculations are almost identical to our PBE results, which suggests that the present results are reliable. It can be clearly seen that the structure seems to be independent of the metal element but increases monotonously with the atomic number of chalcogen. In addition, it can also be found that LDA calculation gives a smaller value than PBE, while the results of PBE and optB88-vdW are almost the same, which are also closer to bulk crystals. This is in agreement with

Table 1. The optimized structural parameters of monolayer TMDCs using LDA, PBE, and optB88-vdW methods. Here, a and d_{x-x} represent the lattice constant and the bond length of two X atoms, respectively. The PBE results from Refs. [13] and [14] are also listed for comparison.

	a/Å					d_{x-x}/Å		
	LDA	PBE	optB88	Ref. [14]	Ref. [13]	LDA	PBE	optB88
MoO_2	2.79	2.83	2.83	2.83	-	2.44	2.47	2.47
MoS_2	3.12	3.18	3.19	3.18	3.18	3.11	3.13	3.14
$MoSe_2$	3.24	3.32	3.32	3.32	3.32	3.31	3.33	3.34
$MoTe_2$	3.46	3.55	3.56	3.54	3.55	3.59	3.61	3.62
WO_2	2.79	2.85	2.83	2.83	-	2.44	2.48	2.48
WS_2	3.12	3.18	3.19	3.18	3.18	3.12	3.14	3.15
WSe_2	3.24	3.32	3.32	3.32	3.32	3.33	3.35	3.36
WTe_2	3.47	3.55	3.56	3.55	3.55	3.6	3.63	3.63

the well accepted knowledge that LDA overestimates the binding of materials. The similar results of PBE and optB88-vdW indicate that van der Waals functional can provide a balanced description for systems dominated by not only vdW force but also covalence bonding, and van der Waals interaction has few effects on such a monolayer TMDCs.

3.1.2. Electronic properties

Now, we focus on band structures of monolayer TMDCs. Since the (semi)-local functionals are known to give a similar band structure for materials, we only give the energy band of monolayer TMDCs calculated using PBE functional. As shown in Fig. 2, all those eight kinds of single layer TMDCs are semiconductors with a distinct band gap, which is quite different from the zero-band-gap graphene. For example, the monolayer MoS_2 has a direct band gap at the K point with a band gap value of 1.62 eV, which is close to the experimental study for atomically thin MoS_2 layers.[4,5] The direct band gap at the K point can also be found in the cases of monolayer $MoSe_2$ and $MoTe_2$, and the corresponding band gaps are 1.44 eV and 1.07 eV, respectively. However, for the case of MoO_2, the band gap is indirect with a value of 0.98 eV. For monolayer MX_2 (where M represents Mo and W) with direct energy gaps, the band gaps decrease when the chalcogenides element becomes heavier i.e., the energy gap order is disulfide>diselenide >ditelluride. To analyze the underlying mechanism, we have performed Bader charge analysis, which is known to be able to get the charge transfer between different atomic species. Taking MoX_2 as an example, we can find the total charges of Mo atom in monolayer MoX_2 are 4.29e, 4.52e, and 5.06e, which suggests that the charges transferred from metal to chalcogen atom are 1.71e, 1.48e, and 0.94e, respectively. This indicates that the reactivity and binding decrease from S to Te, which can also be supported by the fact that the lattice constants decrease with the row number of X in Mo dichalcogenides. Clearly, the strong reactivity of the chalcogen atom will enhance the hybridization, which will lead to a larger band gap of the compounds. In addition, the band gap for MoX_2 (X = Se, S) seems to be smaller than WX_2, and $MoTe_2$ and WTe_2 have quite close gaps. However, for monolayer oxide with indirect-band-gap, the band gap of WO_2 is much larger than that of MoO_2. The calculated band gaps agree well with other studies.[13,27]

3.1.3. Elastic properties

Elastic property is another important physics quantity studied in the present work. For 2D TMDCs, it is possible to measure the elastic constants of these materials from nanoindentation experiments using an atomic force microscope.[28] However, since the experimental measurement suffers from some uncertainness such as defect, the first-principle calculation can offer an important supplement to the experiment.

The elastic constants for monolayer TMDCs calculated with PBE method are reported in Table 2. Since the monolayers of 2H-MX_2 belong to isotropic structures, the linear elastic constant C_{22} is equal to C_{11}. Linear elastic constants of MoX_2 and WX_2 decrease monotonically with the increase of chalcogen's atomic number, which means the decrease of the Young modulus, and for the same chalcogenide atoms, the WX_2 compounds have a larger elastic constant than MoX_2 compounds. The Poisson ratio used to describe the lateral deformation is calculated by $\nu = C_{12}/C_{11}$. It is remarkable that the Poisson ratios of those 2D TMDCs are larger than that of graphene except for WTe_2, which means much better lateral contraction property than graphene. The calculated Poisson ratio for MoS_2 is also close to the results of other studies.[12,14]

For further discussion of elastic properties of those monolayer TMDCs, we also evaluate the Young modulus $E = (C_{11}^2 - C_{12}^2)/C_{11}$. As shown in Table 3, the Young moduli from different methods are close to each other. The values for PBE and optB88-vdW are almost the same, while the results of LDA are larger than others. Although there are some numerical differences, the results of three methods present the same trends that Young moduli decrease with the atomic number of chalcogen and increase from Mo to W compounds. As shown above, charge transfer decreases and lattice constant increases in transition metal dichalcogenides MX_2 when X changes from S to Te, which suggests that the reactivity and binding decrease

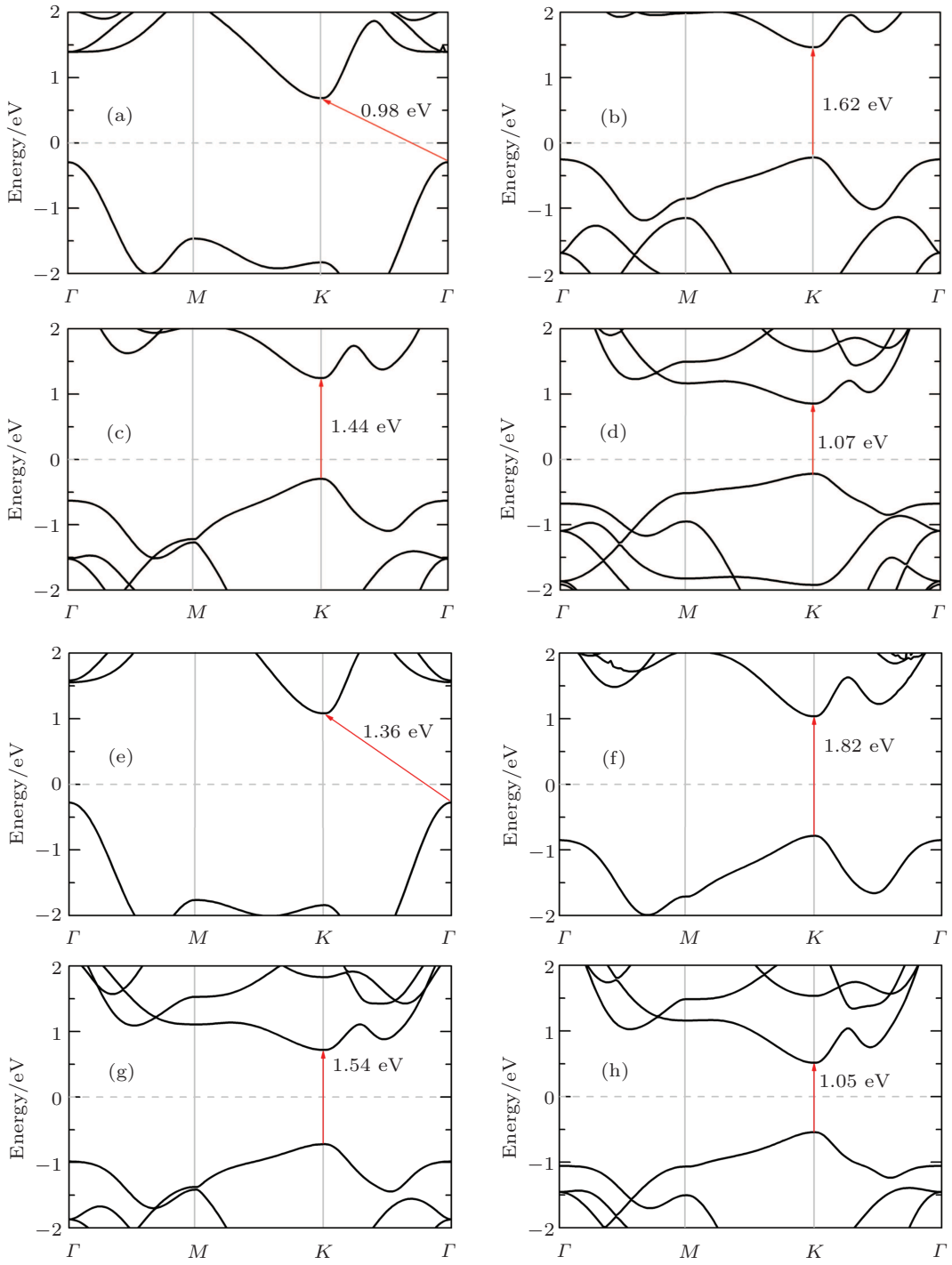


Fig. 2. (color online) The band structures for monolayer TMDCs calculated using PBE. Panels (a)–(h) represent MoO_2, MoS_2, $MoSe_2$, $MoTe_2$, WO_2, WS_2, WSe_2, and WTe_2, respectively. The Fermi energy is marked with light gray dashed lines. The band gaps are shown with red arrows.

Table 2. The calculated elastic constants of monolayer TMDCs in units of $N{\cdot}m^{-1}$ calculated using PBE functional. The data of graphene is also listed for comparison.

	MoO_2	MoS_2	$MoSe_2$	$MoTe_2$	WO_2	WS_2	WSe_2	WTe_2	graphene
C_{11}	232.92	134.89	110.7	84.72	253.25	148.47	122.01	91.42	351.6
C_{12}	84.67	32.03	25.66	20.25	91.32	31.20	22.91	15.40	64.10
C_{44}	74.12	51.43	42.52	32.23	80.96	58.63	43.03	38.01	143.75
ν	0.36	0.24	0.23	0.24	0.36	0.21	0.19	0.17	0.18

from MS_2 to MTe_2. The weakening binding between the metal and the chalcogen atom thus leads to the smaller Young modulus. In addition, we can also find that the Young moduli for those monolayer TMDCs are comparable to that for graphene. For instance, Young moduli for MoO_2 and WO_2 are almost two-thirds of that for the graphene, which is relatively high.

MoS_2, $MoSe_2$, WS_2, and WSe_2 have values about one-third of that for the graphene showing an excellent elastic property. The calculated Young moduli (141 $N{\cdot}m^{-1}$ and 156 $N{\cdot}m^{-1}$) using LDA for monolayer MoS_2 and WS_2 agree well with theoretical results[13,14] and experiment measurement results (180 ± 60 $N{\cdot}m^{-1}$ [9] or around 170 $N{\cdot}m^{-1}$ [10]). We can also find that LDA calculations gave the closest results to experimental results among three functionals, which suggest that LDA calculations are more accurate to describe the elastic property of monolayer TMDCs.

Table 3. The Young moduli of TMDCs in units of $N{\cdot}m^{-1}$ with PBE, LDA, and vdW-DF(optB88-vdW) methods.

	PBE	LDA	optB88
MoO_2	202.1	221.8	199.8
MoS_2	127.3	141.2	123.5
$MoSe_2$	104.8	120.9	105.7
$MoTe_2$	79.9	94.07	80.7
WO_2	220.3	254.3	219.7
WS_2	141.9	156.4	140.7
WSe_2	114.4	132.8	118.2
WTe_2	88.8	101.8	88.4

3.2. Bilayer TMDCs

3.2.1. Structure properties

There are different configurations when monolayers are stacked into bilayer structure.[19] As Fig. 1(c) shows, five stacking orders for the bilayer TMDCs are considered in this paper. Since the optB88-vdW can give a very similar in-plane lattice parameter with PBE and the interlayer interaction is dominated by vdW forces, we only analyze the results of the bilayer TMDCs using optB88-vdW functional. LDA calculation is also performed for comparison. The AA1 and AB with almost degenerate energy are found to be the most stable configuration for all bilayer TMDCs, which also agrees with the earlier calculations.[19] Firstly, we also give the structure parameters with five different stacking orders using LDA and optB88-vdW methods in Table 4. We can find that, the stack of the monolayer does not change the monolayer structure much. The lattice constants of monolayer and bilayer TMDCs are almost the same as these obtained by both LDA and optB88-vdW methods, while the inter-layer distances represented as d_{m-m} varies with the stacking order. Both methods predict that the AA and AB1 stacking order have a larger value of d_{m-m} than other stacking orders, while the distance for AA1 is the smallest, which agrees with the stability order of those configurations. The interlayer distances for bilayer TMDCs range from 5.2 to 7.8 Å according to our calculation. It is clearly shown that the structural parameters including in-plane lattice parameter and inter-layer distance obtained from LDA are much smaller than that of optB88-vdW for the same bilayer structures.

Table 4. The optimized structural parameters of bilayer TMDCs using LDA and optB88-vdW methods. Here, a represents lattice constant, d_{m-m} is the distance of the metal atoms between different layers.

Stacking order		A1B		AA		AA1		AB		AB1	
		a/Å	d_{m-m}/Å	a/Å	d_{m-m}/Å	a/Å	d_{m-m}/Å	a/Å	d_{m-m}/Å	a/Å	d_{m-m}/Å
MoO_2	LDA	2.79	4.81	2.79	5.30	2.79	4.86	2.79	4.82	2.79	5.28
	optB88	2.83	5.28	2.83	5.69	2.83	5.23	2.83	5.20	2.83	5.54
MoS_2	LDA	3.12	6.09	3.12	6.80	3.12	6.01	3.12	5.98	3.12	6.68
	optB88	3.18	6.36	3.19	6.75	3.19	6.28	3.19	6.24	3.19	6.71
$MoSe_2$	LDA	3.25	6.52	3.25	7.05	3.25	6.33	3.25	6.35	3.25	7.05
	optB88	3.33	6.64	3.32	7.14	3.32	6.57	3.33	6.57	3.32	7.09
$MoTe_2$	LDA	3.47	7.08	3.46	7.73	3.47	6.85	3.47	6.89	3.47	7.71
	optB88	3.56	7.25	3.56	7.78	3.56	7.10	3.56	7.11	3.56	7.75
WO_2	LDA	2.79	4.88	2.79	5.34	2.79	4.90	2.79	4.87	2.79	5.31
	optB88	2.83	5.27	2.83	5.68	2.83	5.22	2.83	5.19	2.83	5.58
WS_2	LDA	3.13	6.18	3.13	6.81	3.13	6.06	3.13	6.04	3.12	6.69
	optB88	3.18	6.37	3.19	6.82	3.19	6.29	3.19	6.26	3.19	6.73
WSe_2	LDA	3.25	6.54	3.25	7.14	3.25	6.39	3.25	6.44	3.25	7.1
	optB88	3.33	6.70	3.33	7.15	3.33	6.54	3.33	6.61	3.33	7.14
WTe_2	LDA	3.47	7.13	3.47	7.76	3.47	6.87	3.47	6.95	3.47	7.72
	optB88	3.57	7.27	3.56	7.79	3.56	7.12	3.57	7.12	3.56	7.76

3.2.2. Electronic properties

The band gaps of TMDCs are known to be tunable with thickness.[5,10,29] It is thus interesting to investigate the electronic structure of bilayer TMDCs. Since the low-energy AA1 and AB are found to have similar band structures, we only give the band structures of bilayer TMDCs in AA1 stacking order in Fig. 3. Unlike the direct band gap of monolayers, indirect

band gap is found except for bilayer WTe_2 which still has a direct band gap at the K points as shown in Fig. 3(h). We can easily find that the band gaps have the same variation behavior as the monolayers from MO_2 to MTe_2. It has to be mentioned that the valence-band maximum (VBM) of bilayer WTe_2 at K point is only 0.06 eV larger than the maximum energy for Γ point, which is much smaller than energy difference in other cases. When monolayers are stacked into bilayers, the band gaps were found to decrease, which agrees well with previous theoretical studies.[19,30]

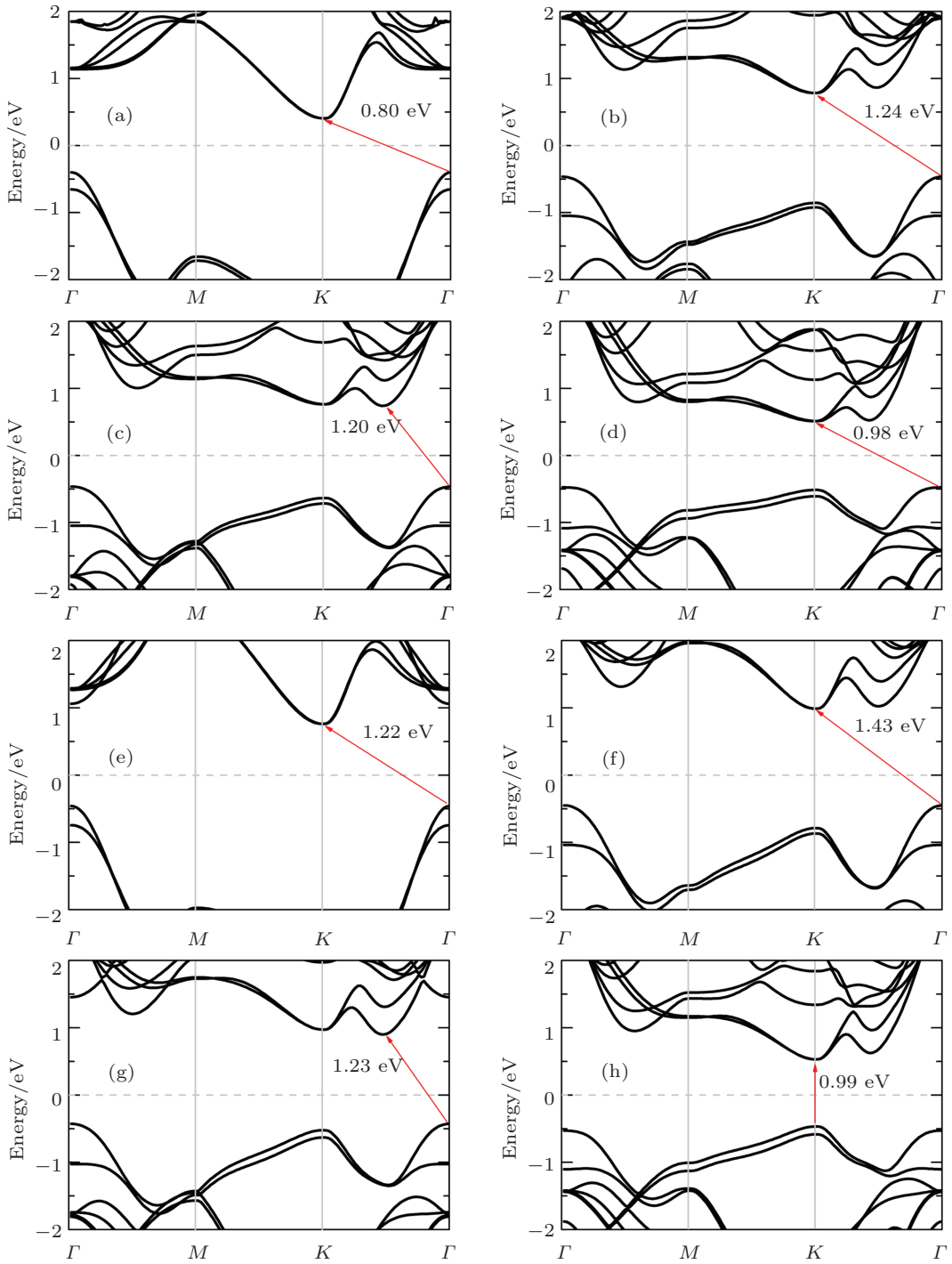


Fig. 3. (color online) The band structures for monolayer TMDCs calculated using PBE. Panel (a)–(h) represents MoO_2, MoS_2, $MoSe_2$, $MoTe_2$, WO_2, WS_2, WSe_2, and WTe_2, respectively. The Fermi energy is marked with light gray dashed lines. The band gaps are shown with red arrows.

3.2.3. Elastic properties

To reveal the evolution of mechanical properties of TMDCs with thickness, we also calculated the elastic constants, Young modulus, and Poisson ratio of bilayer TMDCs in Table 5. The trend of bilayer Young modulus is very similar to that of monolayers. A decrease of Young modulus is found from MO_2 to MTe_2 and the Young modulus of WX_2 is

larger than that of MoX_2. The Young moduli of AA and AB1 stacking orders are found to be larger than the others according to LDA. Meanwhile, we also find the differences of Young moduli for different stacking orders are within 5%, which indicates that the stacking order has little influence on the elastic properties of the bilayer. Compared with optB88-vdW functional, LDA has a larger Young modulus. In particular, LDA method predicts the Young moduli of around 280 N·m^{-1} for bilayer MoS_2, which is consistent with the recent experiment 300±13 N·m^{-1}.[10] Table 5 also shows the Poisson ratios of bilayers of TMDCs with different configurations. The calculated results show that these bilayers have close Poisson ratios to the corresponding monolayer. Among different TMDCs bilayer, MoS_2, $MoSe_2$, and $MoTe_2$ have similar Poisson ratios with the value of 0.2, which is also independent of the stacking order, while the Poisson ratios for bilayer WSe_2 and WTe_2, are found to be much smaller than that of the others. We also notice that optB88-vdW predicts larger Poisson ratios than LDA.

It should be noticed that the inter-layer interaction is known to be predominated by vdW interaction, an accurate description for such a system may need a more advanced treatment such as RPA. However, on the basis of the reasonable description for elastic properties of TMDCs, LDA method may be an alternative to describe the elastic properties of bilayer TMDCs. Recently, Liu *et al.*[10] have investigated the elastic modulus of CVD grown monolayer MoS_2 and WS_2 and their bilayer heterostructures and found that the 2D moduli of their bilayer heterostructures are lower than the sum of 2D modulus of each layer, which shows a strong mechanical interlayer coupling between the layers. However, according to the present results, the Young modulus of bilayer structure calculated by both LDA and optB88-vdW is almost twice that of the corresponding monolayer, which shows that the mechanical coupling between monolayers seems to be negligible in bilayers. Considered the experimental uncertainty, further effort both in experimental and theory is thus suggested to investigate the mechanical coupling of monolayers in bilayer.

Table 5. Young moduli and Poisson ratios for bilayer TMDCs with different stacking orders.

Young modulus/N·m^{-1}	A1B		AA		AA1		AB		AB1	
	LDA	optB88	LDA	optB88	LDA	optB88	LDA	optB88	LDA	optB88
MoO_2	439.7	400.7	442.3	399.9	439.4	398.9	438.9	399.8	441.2	405.5
MoS_2	281.9	255.7	285.9	249.9	282.0	252.2	276.4	254.0	283.2	248.2
$MoSe_2$	236.9	210.4	241.1	213.4	238.2	212.8	236.1	212.2	240.7	213.7
$MoTe_2$	182.9	163.0	189.0	167.7	186.6	162.0	182.1	158.6	186.8	161.7
WO_2	503.4	461.9	509.1	470.8	504.2	471.1	503.9	468.9	509.6	461.9
WS_2	314.1	291.7	313.2	279.6	309.7	282.2	309.9	280.7	313.7	282.3
WSe_2	262.2	232.4	265.7	233.2	265.1	227.3	262.5	234.3	266.1	232.5
WTe_2	198.8	172.5	204.1	177.9	203.2	175.9	200.1	172.3	202.9	176.9
Poisson ratio	A1B		AA		AA1		AB		AB1	
	LDA	optB88	LDA	optB88	LDA	optB88	LDA	optB88	LDA	optB88
MoO_2	0.365	0.364	0.366	0.367	0.365	0.367	0.369	0.37	0.365	0.353
MoS_2	0.212	0.239	0.199	0.253	0.227	0.247	0.218	0.234	0.222	0.256
$MoSe_2$	0.201	0.224	0.205	0.232	0.214	0.230	0.211	0.223	0.209	0.229
$MoTe_2$	0.202	0.221	0.210	0.218	0.213	0.242	0.217	0.248	0.212	0.245
WO_2	0.342	0.348	0.337	0.331	0.336	0.329	0.341	0.332	0.340	0.348
WS_2	0.180	0.194	0.195	0.220	0.201	0.219	0.198	0.213	0.197	0.216
WSe_2	0.173	0.191	0.179	0.200	0.174	0.217	0.174	0.189	0.175	0.204
WTe_2	0.154	0.193	0.155	0.188	0.159	0.199	0.160	0.201	0.158	0.189

4. Conclusion

We have investigated the band structure and elastic properties for eight kinds of two-dimensional TMDCs in monolayer and different bilayers using different functionals. Our results indicate that all those monolayers and bilayers belong to semiconductors and there is a transition from direct gaps for monolayers (except for MoO_2 and WO_2), into indirect gaps in bilayers (except WTe_2). The calculation also shows that the monolayer TMDCs present excellent elastic properties, which are comparable to graphene. Meanwhile, we also find that the LDA method is an efficient alternative to more advanced methods in describing the elastic properties of both monolayer and bilayer TMDCs. Furthermore, our results also show that the elastic property is only influenced slightly by stacking order and the mechanical coupling between monolayers seems to be negligible.

References

[1] Novoselov K S, Geim A K, Morozov S V, Jiang D, Zhang Y, Dubonos S V, Grigorieva I V and Firsov A A 2004 *Science* **306** 666

[2] Chen J H, Jang C, Xiao S, Ishigami M and Fuhrer M S 2008 *Nat. Nanotechnol.* **3** 206

[3] Lee C, Wei X, Kysar J W and Hone J 2008 *Science* **321** 385

[4] Splendiani A, Sun L, Zhang Y, Li T, Kim J, Chim C Y and Galli G and Wang F 2010 *Nat. Nanotechnol.* **10** 1271
[5] Mak K F, Lee C, Hone J, Shan J and Heinz T F 2010 *Phys. Rev. Lett.* **105** 136805
[6] Wang Q H, Kalantar-Zadeh K, Kis A, Coleman J N and Strano M S 2012 *Nat. Nanotechnol.* **7** 699
[7] Xu X, Yao W, Xiao D and Heinz T F 2014 *Nat. Phys.* **10** 343
[8] Geim A K and Grigorieva I V 2013 *Nature* **499** 419
[9] Bertolazzi S, Brivio J and Kis A 2011 *ACS Nano* **5** 9703
[10] Liu K, Yan Q, Chen M, Fan W, Sun Y, Suh J, Fu D, Lee S, Zhou J, Tongay S, Ji J, Neaton J B and Wu J 2014 *Nano Lett.* **14** 5097
[11] Ataca C, Topsakal M, Akturk E and Ciraci S 2011 *J. Phys. Chem. C* **115** 16354
[12] Cooper R C, Lee C, Marianetti C A, Wei X, Hone J and Kysar J W 2013 *Phys. Rev. B* **87** 035423
[13] Kang J, Tongay S, Zhou J, Li J and Wu J 2013 *Appl. Phys. Lett.* **102** 012111
[14] Çakr D, Peeters F M and Sevik C 2014 *Appl. Phys. Lett.* **104** 203110
[15] Wang Z Y, Zhou Y L, Wang X Q, Wang F, Sun Q, Guo Z X and Jia Y 2015 *Chin. Phys. B* **24** 026501
[16] Molina-Sánchez A, Sangalli D, Hummer K, Marini A and Wirtz L 2013 *Phys. Rev. B* **88** 045412
[17] Yun W S, Han S W, Hong S C, Kim I G and Lee J D 2012 *Phys. Rev. B* **85** 033305
[18] Ramasubramaniam A, Naveh D and Towe E 2011 *Phys. Rev. B* **84** 205325
[19] He J, Hummer K and Franchini C 2014 *Phys. Rev. B* **89** 075409
[20] Kresse G and Hafner J 1993 *Phys. Rev. B* **47** 558
[21] Kresse G and Furthmüller J 1996 *Phys. Rev. B* **54** 11169
[22] Klimeš J, Bowler D R and Michaelides A 2010 *J. Phys.: Condens. Matter* **22** 022201
[23] Klimeš J, Bowler D R and Michaelides A 2011 *Phys. Rev. B* **83** 195131
[24] Zhang W B, Chen C and Tang P Y 2014 *J. Chem. Phys.* **141** 044708
[25] Cadelano E, Palla P L, Giordano S and Colombo L 2010 *Phys. Rev. B* **82** 235414
[26] Ataca C and Ciraci S 2011 *J. Phys. Chem. C* **115** 13303
[27] Shi H, Pan H, Zhang Y W and Yakobson B I 2013 *Phys. Rev. B* **87** 155304
[28] Castellanos-Gomez A, Poot M, Steele G A, van der Zant H S, Agraït N and Rubio-Bollinger G 2012 *Adv. Mater.* **24** 772
[29] Conley H J, Wang B, Ziegler J I, Haglund Jr R F, Pantelides S T and Bolotin K I 2013 *Nano Lett.* **13** 3626
[30] Ataca C, Sahin H and Ciraci S 2012 *J. Phys. Chem. C* **116** 8983